

Effects of Dopant Concentrations on Thin Films with Coherent Formulation at Visible Wavelengths

¹M. Omidpanah and ²S.A.A. Oloomi

¹Department of Mechanical Engineering, Technical and Vocational University, Yazd, Iran

²Department of Mechanical Engineering, Yazd Branch, Islamic Azad University, Yazd, Iran

(Received: April 24, 2012; Accepted: August 23, 2012)

Abstract: Semiconductor materials with coatings have a wide range of applications in MEMS and NEMS. This work uses transfer-matrix method for calculating the radiative properties. Doped silicon is used and the coherent formulation is applied. The Drude model for the optical constants of doped silicon is employed. Results showed that for the visible wavelengths, more emittance occurs in high concentrations and the reflectance decreases as the concentration increases. In these wavelengths, transmittance is negligible. Donors and acceptors act similar in visible wavelengths. The effect of wave interference can be understood by plotting the spectral properties such as reflectance or transmittance of a thin dielectric film versus the film thickness and analyzing the oscillations of properties due to constructive and destructive interferences. But this effect has not been shown at visible wavelengths. At room temperature, the scattering process is dominated by lattice scattering for lightly doped silicon and the impurity scattering becomes important for heavily doped silicon when the dopant concentration exceeds 10^{18} cm^{-3} .

Key words: Dopant; concentrations-radiative; properties-nanoscale; multilayer-coherent; formulation-visible wavelengths

INTRODUCTION

Understanding the radiative properties of semiconductors is essential for the advancement of manufacturing technology, such as rapid thermal processing [1]. Because of the major heating source in rapid thermal processing is lamp radiation, knowledge of radiative properties is important for temperature control during the process.

Silicon is semiconductor that plays a vital role in integrated circuits and MEMS/NEMS [2]. Semitransparent crystalline silicon solar cells can improve the efficiency of solar power generation [3]. Accurate radiometric temperature measurements of silicon wafers and heat transfer analysis of rapid thermal processing furnaces require a thorough understanding of the radiative properties of the silicon wafer, whose surface may be coated with dielectric or absorbing films [1]. In fact, surface modification by coatings can significantly affect the radiative properties of a material [4].

Oloomi *et al.* [2] have showed for lightly doped silicon that silicon dioxide coating has higher reflectance than silicon nitride coating for visible wavelengths. In visible wavelengths the reflectance

increases as the temperature increase. That was due to decrease in emittance; but in infrared wavelengths the reflectance and transmittance decrease as the temperature increases [2, 5].

This work uses transfer-matrix method for calculating the radiative properties. Doped silicon is used and the coherent formulation is applied. The Drude model for the optical constants of doped silicon is employed. In this work, phosphorus and boron are default impurities for n-type and p-type, respectively.

MODELING

Coherent formulation: When the thickness of each layer is comparable or less than the wavelength of electromagnetic waves, the wave interference effects inside each layer become important to predict correctly the radiative properties of multilayer structure of thin films. The transfer-matrix method provides a convenient way to calculate the radiative properties of multilayer structures of thin films (Fig. 1).

Assuming that the electromagnetic field in the j th medium is a summation of forward and backward waves in the z -direction, the electric field in each layer can be expressed by the following relations:

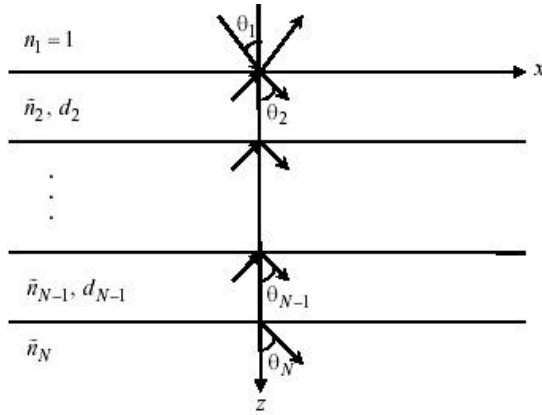


Fig. 1: The geometry for calculating the radiative properties of a multilayer structure

$$E_j = \begin{cases} [A_1 e^{iq_1 z} + B_1 e^{-iq_1 z}] e^{(iq_x x - i\omega t)}, j=1 \\ [A_j e^{iq_{jz}(z-z_{j-1})} + B_j e^{-iq_{jz}(z-z_{j-1})}] e^{(iq_x x - i\omega t)}, j=2,3,\dots,N \end{cases} \quad (1)$$

where A_j and B_j are the amplitudes of forward and backward waves in the j th layer. Detailed descriptions of how to solve for A_j and B_j is given in [6].

THE DRUDE MODEL FOR THE OPTICAL CONSTANTS OF DOPED SILICON

The complex dielectric function is related to the refractive index (n) and the extinction coefficient (κ) by this equation

$$\epsilon(\omega) = (n + i\kappa)^2 \quad (2)$$

To account for the doping effects, the Drude model is employed and the dielectric function of both intrinsic and doped silicon is expressed as the following form [7]:

$$\epsilon(\omega) = \epsilon_{bl} - \frac{N_e e^2 / \epsilon_0 m_e^*}{\omega^2 + i\omega / \tau_e} - \frac{N_h e^2 / \epsilon_0 m_h^*}{\omega^2 + i\omega / \tau_h} \quad (3)$$

where the first term in the right (ϵ_{bl}) accounts for contributions by transitions across the band gap and lattice vibrations, the second term is Drude term for transitions in the conduction band (free electrons) and the last term is Drude term for transitions in the valence band (free holes). Here, N_e and N_h are the concentrations, m_e^* and m_h^* the effective masses, τ_e and τ_h the scattering times for free electrons and holes, respectively and e is the electron charge. For

simplicity, the effective masses are assumed to be independent of the frequency, dopant concentration and temperature in the present study and their values are extracted from literature [8] as state below:

$$m_e^* = 0.27m_0 \quad (4)$$

$$m_h^* = 0.37m_0 \quad (5)$$

where m_0 is the electron mass in vacuum. Since ϵ_{bl} accounts for all contributions other than the free carriers, it can be determined from the refractive index and extinction coefficient of silicon as [1].

$$\epsilon_{bl} = (n_{bl} + i\kappa_{bl})^2 \quad (6)$$

When considering the contribution from transitions across the band gap, the modification of the band structure by impurities is neglected and this assumption should not cause significant error [7]. In this work, the expression of Jellison and Modine [9] is used to calculate the refractive index n_{bl} in the wavelength region from 0.5 to 0.84 μm .

$$n_{bl}(\lambda, T) = n_0(\lambda) + \beta(\lambda)T \quad (7)$$

$$n_0 = \sqrt{4.565 + \frac{97.3}{3.648^2 - (1.24/\lambda)^2}} \quad (8)$$

$$\beta(\lambda) = -1.864 \times 10^{-4} + \frac{5.394 \times 10^{-3}}{3.648^2 - (1.24/\lambda)^2} \quad (9)$$

the extinction coefficient κ_{bl} counts for the band gap absorption as well as the lattice absorption. The band gap absorption occurs when the photon energy is greater than the band gap energy of silicon and results in a large absorption coefficient. The absorption coefficient is related to the extinction coefficient as follows:

$$\alpha = 4\pi\kappa / \lambda \quad (10)$$

where κ_{bl} can be determined for all temperatures from the equation for absorption coefficients. In this paper the extinction coefficient of silicon is calculated from Jellison and Modine's expression in the wavelength range from 0.4 to 0.9 μm [9].

$$\kappa_{bl}(\lambda, T) = k_0(\lambda) \exp \left[\frac{T}{369.9 - \exp(-12.92 + 6.831/\lambda)} \right] \quad (11)$$

$$k_0(\lambda) = -0.0805 + \exp \left[-3.1893 + \frac{7.946}{3.648^2 - (1.24/\lambda)^2} \right] \quad (12)$$

Once ϵ_{bl} is determined from the preexisting functional expressions and tabulated data, the remaining parameters are the carrier concentrations and scattering times, which are functions of the temperature and dopant concentration. The calculation of carrier concentrations requires the knowledge of the Fermi energy (E_F). By knowing the Fermi energy, carrier concentrations can be obtained from the following equations [10]:

$$N_e = N_C F_{1/2} \left(\frac{E_F - E_g}{kT} \right) \quad (13)$$

$$N_h = N_V F_{1/2} \left(\frac{-E_F}{kT} \right) \quad (14)$$

where N_C and N_V are the effective density of states in the conduction and valence band, respectively, $F_{1/2}$ is a Fermi-Dirac integral of order 1/2, E_g is the band gap energy and given below [11]:

$$E_g = 1.17 - 0.000473T^2 / (T + 636) \text{eV} \quad (15)$$

k is Boltzmann's constant. The values for the effective density of states at room temperature are reported in literature [12] as follows:

$$N_C = 2.86 \times 10^{19} \text{cm}^{-3} \quad (16)$$

$$N_V = 2.66 \times 10^{19} \text{cm}^{-3} \quad (17)$$

The Fermi-Dirac integral $F_{1/2}$ can be simplified by an exponential and the procedures described in literature [25] are used to determine Fermi energy satisfying charge neutrality, which is expressed as follows:

$$N_h + N_D^+ = N_e + N_A^- \quad (18)$$

where N_D^+ and N_A^- are ionized donor and acceptor concentration, respectively. In the calculation of carrier concentrations, the ionization energy of the considered impurity or dopant is required. In this work, phosphorus and boron are default impurities for n-type and p-type, respectively.

The ionization energies of phosphorus and boron are assumed to be independent of dopant concentration and temperature and their values are extracted from literature [13] as 44 meV and 45 meV, respectively.

The scattering time τ_e or τ_h depends on the collisions of electrons or holes with lattice (phonons)

and ionized dopant sites (impurities or defects); hence, it generally depends on the temperature and dopant concentration. The total scattering time (for the case of τ_e), which consists of the above two mechanisms, can be expressed as follows [13]:

$$\frac{1}{\tau_e} = \frac{1}{\tau_{e-l}} + \frac{1}{\tau_{e-d}} \quad (19)$$

where τ_{e-l} and τ_{e-d} denote the electron-lattice and electron-defect scattering time, respectively.

Similarly, τ_h can be related to τ_{h-l} and τ_{h-d} . In addition, the scattering time t is also related to the mobility μ by

$$\tau = m^* \mu / e \quad (20)$$

At room temperature, the total scattering time τ_e^0 or τ_h^0 , which depends on the dopant concentration, can be determined from the fitted mobility equations [14]

$$\mu_e^0 = \frac{1268}{1 + (N_D / 1.3 \times 10^{17})^{0.91}} + 92 \quad (21)$$

$$\mu_h^0 = \frac{447.3}{1 + (N_A / 1.9 \times 10^{17})^{0.76}} + 47.7 \quad (22)$$

where superscript 0 indicates values at 300 K and N_D or N_A is the dopant concentration of donor (phosphorus, n-type) or acceptor (boron, p-type) in cm^{-3} . On the other hand, the scattering time from lattice contribution τ_{e-l}^0 or τ_{h-l}^0 , which is independent of the dopant concentration, can be separately obtained from the room temperature lattice mobility of $1451 \text{cm}^2 \cdot \text{V}^{-1} \cdot \text{s}^{-1}$ for electrons or $502 \text{cm}^2 \cdot \text{V}^{-1} \cdot \text{s}^{-1}$ for holes [15]. Consequently, the scattering time from impurity contribution τ_{e-d}^0 or τ_{h-d}^0 can be determined from Equation. (19) by knowing the total scattering time and that due to lattice contribution. At room temperature, the scattering process is dominated by lattice scattering for lightly doped silicon and the impurity scattering becomes important for heavily doped silicon when the dopant concentration exceeds 10^{18}cm^{-3} .

Because of the relatively insignificance of impurity scattering at high temperatures, the following formula will be used to calculate the impurity scattering times:

$$\frac{\tau_{e-d}}{\tau_{e-d}^0} = \frac{\tau_{h-d}}{\tau_{h-d}^0} = \left(\frac{T}{300} \right)^{1.5} \quad (23)$$

In order to obtain a better agreement with the measured near-infrared absorption coefficients for lightly doped silicon [1, 7, 16-18], the expressions for lattice scattering are modified in the present study, as follows:

$$\tau_{e-1} = \tau_{e-1}^0 (T/300)^{-3.8} \quad (24)$$

$$\tau_{h-1} = \tau_{h-1}^0 (T/300)^{-3.6} \quad (25)$$

RESULTS

Consider the case in which the silicon wafer is coated with a silicon dioxide layer on both sides. The thickness of silicon wafer is $500\mu\text{m}$ and the temperature of silicon wafer with thin-film coatings is 25°C and the Electromagnetic waves are incident at $\theta = 0^\circ$. The considered wavelength range is $0.5\mu\text{m} < \lambda < 0.7\mu\text{m}$. Doped silicon is used and the coherent formulation is applied. The thickness of SiO_2 is 400 nm . The Drude model for the optical constants of doped silicon is employed. The optical constants of silicon dioxide and silicon nitride are mainly based on the data collected in Palik's handbook [19, 20]. Phosphorus acts as donar (n-type) and born acts as acceptor (p-type) for doped silicon. The results are categorized for n-type shown in Fig. 2 and 3; while the illustrated data for p-type are shown in Fig. 4 and 5. of present study are shown in Fig. 2-10.

Figure 2a shows the spectral reflectance of silicon wafer coated by silicon dioxide film on both sides with

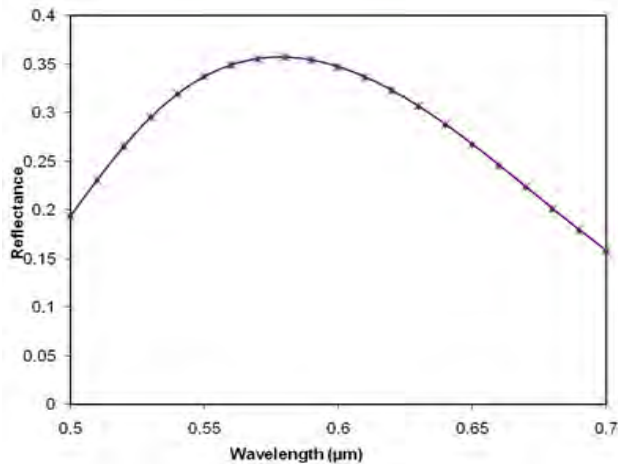


Fig. 2a: Spectral reflectance of silicon wafer coated with silicon dioxide film on both sides with doped silicon (n-type) in different concentrations, at room temperatures and normal incidence for visible wavelengths

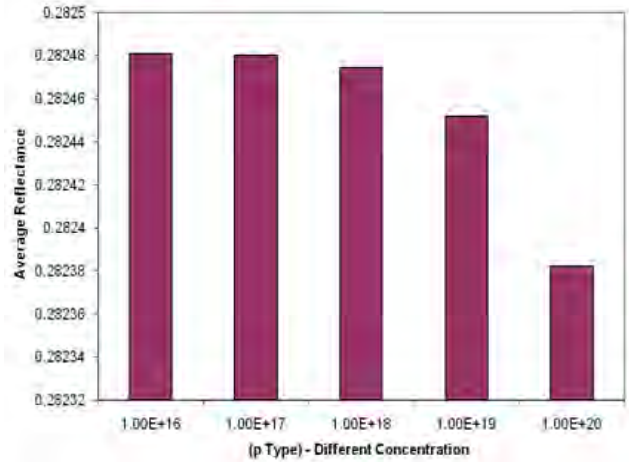


Fig. 2b: Average Reflectance of silicon wafer coated by silicon dioxide film on both sides with doped silicon (n-type) in different concentrations, at room Temperatures and normal incidence for visible wavelengths

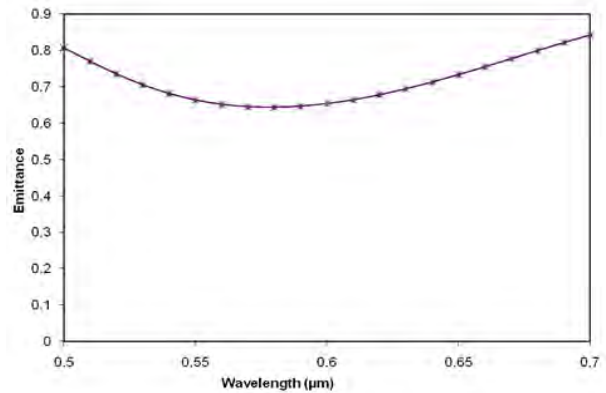


Fig. 3a: Spectral Emittance of silicon wafer coated with silicon dioxide film on both sides with doped silicon (n-type) in different concentrations, at room temperatures and normal incidence for visible wavelengths

doped silicon (n-type) in different concentrations, at room Temperatures and normal incidence for visible wavelength. The maximum reflectance was obtained at wavelength of $0.58\mu\text{m}$.

Figure 2b depicts the average reflectance of silicon wafer coated with silicon dioxide film on both sides with doped silicon (n-type) in different concentrations, at room temperatures and normal incidence for visible wavelengths. At low concentration, the average reflectance values were higher than the n-type high concentration.

Figure 3a depicts the spectral emittance of silicon wafer coated with silicon dioxide film on both sides

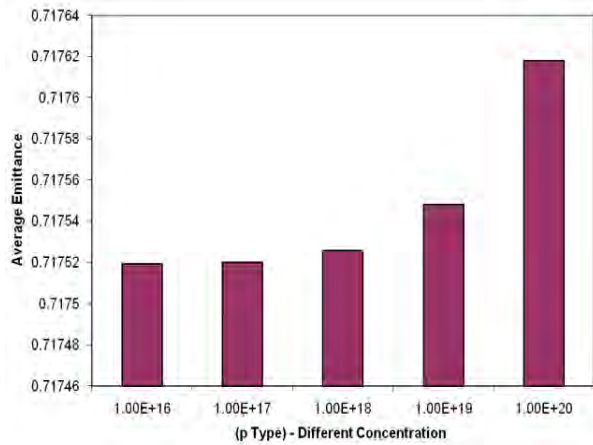


Fig. 3b: Average emittance of silicon wafer coated by silicon dioxide film on both sides with doped silicon (n-type) in different concentrations, at room Temperatures and normal incidence for visible wavelengths

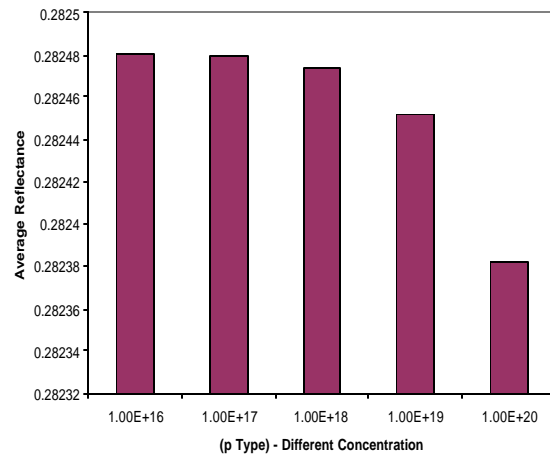


Fig. 4b: Average Reflectance of silicon wafer coated by silicon dioxide film on both sides with doped silicon (p-type) in different concentrations, at room Temperatures and normal incidence for visible wavelengths

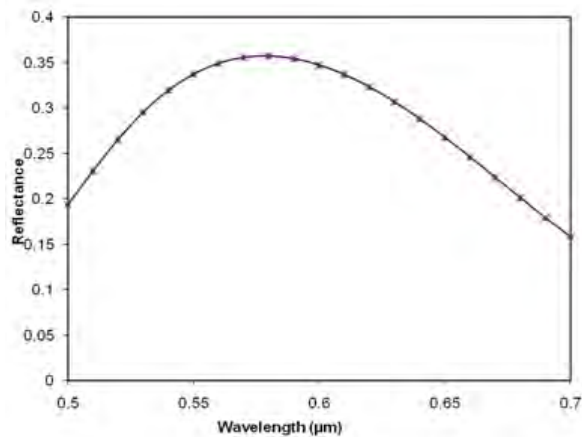


Fig. 4a: Spectral Reflectance of silicon wafer coated by silicon dioxide film on both sides with doped silicon (p-type) in different concentrations, at room Temperatures and normal incidence for visible wavelengths

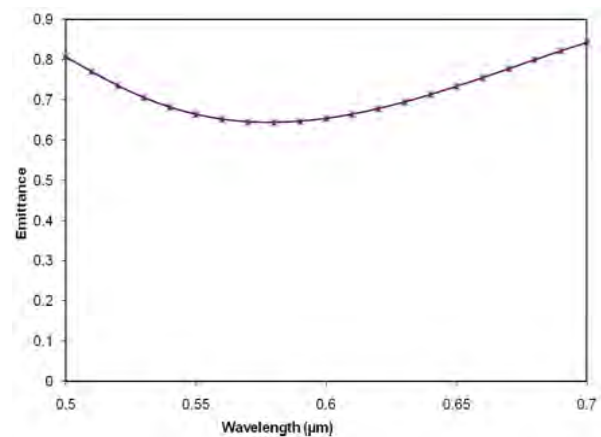


Fig. 5a: Spectral Emittance of silicon wafer coated by silicon dioxide film on both sides with doped silicon (p-type) in different concentrations, at room Temperatures and normal incidence for visible wavelengths

with doped silicon (n-type) in different concentrations, at room temperatures and normal incidence for visible wavelengths. The lowest emittance was obtained at wavelength of 0.58 μm.

The average emittance of silicon wafer coated with silicon dioxide film on both sides with doped silicon (n-type) in different concentrations, at room Temperatures and normal incidence for visible wavelengths is shown in Fig. 3b. Low emittance was obtained at low concentrations.

Similarly the reflectance data for p-types are shown in Fig. 4a. The average reflectance data are

illustrated in Fig. 4b. Data for lambda for difference concentrations were very close; almost were identical; therefore it was not possible to present all data in these figures.

As emittance data are illustrated in Fig. 5a for p-type; the average emittances are shown in Fig. 5b.

Figure 6 the spectral transmittance of silicon wafer coated by silicon dioxide film on both sides with doped silicon (p-type) with lambda values at different concentrations, at room temperatures and normal incidence for visible wavelengths are shown.

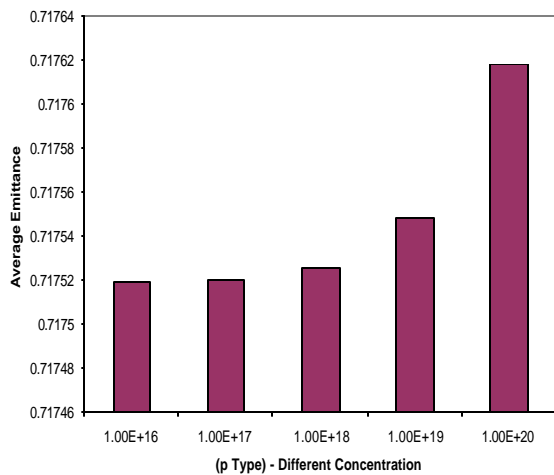


Fig. 5b: Average Emittance of silicon wafer coated by silicon dioxide film on both sides with doped silicon (p-type) in different concentrations, at room Temperatures and normal incidence for visible wavelengths

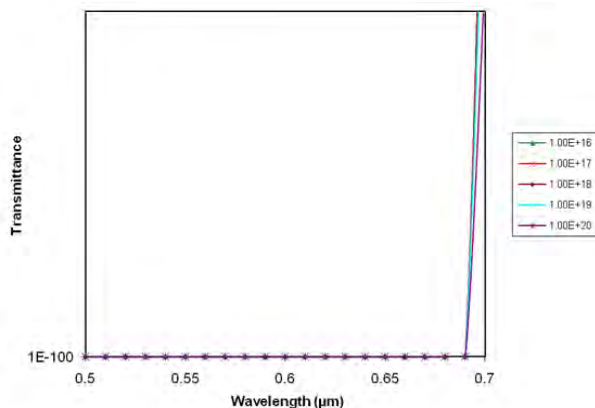


Fig. 6: Spectral Transmittance of silicon wafer coated by silicon dioxide film on both sides with doped silicon (p-type) in different concentrations, at room Temperatures and normal incidence for visible wavelengths

CONCLUSIONS

The effect of wave interference can be understood by plotting the spectral properties such as reflectance or transmittance of a thin dielectric film versus the film thickness and analyzing the oscillations of properties due to constructive and destructive interferences [2, 5].

For visible wavelengths, more emittance occurs in greater concentrations and the reflectance decreases as the concentration increases. In these wavelengths, transmittance is negligible.

Donors and acceptors act similar in visible wavelengths.

At room temperature for concentration less than 10^{19}cm^{-3} , concentration has not important influence on radiative properties. At room temperature, the scattering process is dominated by lattice scattering for lightly doped silicon and the impurity scattering becomes important for heavily doped silicon when the dopant concentration exceeds 10^{18}cm^{-3} .

REFERENCES

1. Timans, P.J., 1996. The thermal radiative properties of semiconductors. Advances in Rapid Thermal and Integrated Processing. Academic Publishers, Dordrecht, Netherlands, pp: 35-102.
2. Oloomi, S.A.A, A. Sabounchi and A. Sedaghat, 2008. Predict Thermal Radiative Properties of Nanoscale Multilayer Structures. The IASTED International Conference on Nanotechnology and Applications. Crete-Greece.
3. Fath, P., H. Nussbaumer and R. Burkhardt, 2002. Industrial manufacturing of semitransparent crystalline silicon power solar cells. Sol Energy Mater Sol Cells, 74: 127-131.
4. Makino, T., 2002. Thermal radiation spectroscopy for heat transfer science and for engineering surface diagnosis. In: Taine, J., (Eds.). Heat transfer, Oxford: Elsevier Science, 1: 55-66.
5. Oloomi, S.A.A., A. Sabounchi and A. Sedaghat, 2009. Computing Thermal Radiative Properties of Nanoscale Multilayer. The International Conference on Computer Science and Engineering, Dubai, United Arab Emirates.
6. Fu, C.J, Z.M. Zhang and Q.Z. Zhu, 2003. Optical and Thermal Radiative Properties of Semiconductors Related to Micro/Nanotechnology. Advanced in Heat Transfer, 37: 179-296.
7. Hebb, J.P., 1997. Pattern Effects in Rapid Thermal Processing. Ph.D. Dissertation, Department of Mechanical Engineering, Massachusetts Institute of Technology, Cambridge, MA.
8. Spitzer, W.G. and H.Y. Fan, 1957. Determination of Optical Constants and Carrier Effective Mass of Semiconductors. Phys. Rev., 1: 882-890.
9. Jellison, G.E. and F.A. Modine, 1994. Optical Functions of Silicon at Elevated Temperatures. J. Appl. Phys., 76 : 3758-3761.
10. Gaylord, T.K. and J.N. Linxwiler, 1976. A Method for Calculating Fermi Energy and Carrier Concentrations in Semiconductors. Am. J. Phys., 44: 353-355.

11. Thurmond, C.D., 1975. Standard Thermodynamic Functions for Formation of Electrons and Holes in Ge, Si, GaAs and Gap. *J. Electrochem. Soc.*, 122: 1133-1141.
12. Sze, S.M., 2002. *Semiconductor Devices. Physics and Technology*, 2nd Ed., Wiley, New York.
13. Sze, S.M., 1981. *Physics of Semiconductor Devices*. 2nd Ed., Wiley, New York.
14. Beadle, W.E., J.C.C. Tsai and R.D. Plummer, 1985. *Quick Reference Manual for Silicon Integrated Circuit Technology*. Wiley, New York.
15. Morin, F.J. and J.P. Maita, 1954. Electrical Properties of Silicon Containing Arsenic and Boron. *Phys. Rev.*, 96: 28-35.
16. Sturm, J.C. and C.M. Reaves, 1992. Silicon Temperature-Measurement by Infrared Absorption-Fundamental Processes and Doping Effects. *IEEE Trans. Electron Devices*, 39: 81-88.
17. Vandenabeele, P. and K. Maex, 1992. Influence of Temperature and Backside Roughness on the Emissivity of Si Wafers During Rapid Thermal-Processing. *J. Appl. Phys.*, 72: 5867-5875.
18. Rogne, H., P.J. Timans and H. Ahmed, 1996. Infrared Absorption in Silicon at Elevated Temperatures. *Appl. Phys. Lett.*, 69: 2190-2192.
19. Palik, E.D., 1998. Silicon Dioxide (SiO₂). *Handbook of Optical Constants of Solids*, San Diego, CA., pp: 749-763.
20. Palik, E.D., 1998. Silicon Nitride (Si₃N₄). *Handbook of Optical Constants of Solids*, San Diego, CA, pp: 771-774.